JOURNAL OF SOLID STATE CHEMISTRY 73, 192–205 (1988)

Electron Microscopic Study of the Homologous Series of Mixed Layer Compounds $As_2Te_3(GeTe)_n$

S. KUYPERS, G. VAN TENDELOO, J. VAN LANDUYT, AND S. AMELINCKX*

RUCA, Universiteit Antwerpen, Groenenborgerlaan 171, B 2020 Antwerpen, Belgium

AND HAN WAN SHU, S. JAULMES, J. FLAHAUT, AND P. LARUELLE

Université René Descartes, 4, Avenue de l'Observatoire, F 75270 Paris, France

Received March 19, 1987; in revised form June 29, 1987

The mixed layer compounds $As_2Te_3(GeTe)_n$ form a homologous series. Their structure consists of lamellae of close-packed layers containing n layers of GeTe alternating with single layer lamellae of As_2Te_3. Their structure, first determined by means of X-rays for the compound $n = 5$, is confirmed by means of electron diffraction and high-resolution electron microscopy for the whole series of compounds up to $n = 9$. In the higher members ($n > 9$) the arsenic layers occur in a nonperiodic way. © 1988 Academic Press, Inc.

I. Introduction

The structures of several members of the series of compounds $As_2Ge_nTe_{3+n}$ have recently been determined by Han Wan Shu *et al.* (*1*) using X-ray diffraction methods. The crystal structures of these compounds of which the chemical composition can be written as $(As_2Te_3)(GeTe)_n$ are very closely related; they form a homologous series.

The authors propose a phase diagram based on their X-ray results and suggest that the same structural principle should be valid for the whole series extending up to $n = 15$. For the higher members of the series $n > 9$ these results were essentially based on the observed systematic shifts of powder diffraction lines in Guinier patterns.

However, with increasing n value the difference in composition between successive members of the homologous series becomes increasingly smaller and consequently it becomes increasingly more difficult to obtain single crystals of a sufficient size to perform X-ray structure determinations; the authors therefore had to rely on powder patterns for the study of the higher members. As a result it is of interest to study such compounds by means of electron diffraction and electron microscopy whereby small crystal fragments can be examined.

2. Experimental

Materials with compositions corresponding to n values such that $5 < n < 18$ were

* Additional affiliation: SCK/CEN, B 2400 Mol, Belgium.

0022-4596/88 $3.00

prepared by heating the constituent elements in sealed quartz tubes, first at 800°C for 5–8 hr and subsequently for 2 weeks at 350°C.

Samples for examination in the electron microscope were obtained by crushing the material; copper grids covered with glue were subsequently dipped in the crushed powder. The specimens so obtained were not entirely satisfactory. Because of the pronounced basal cleavage it was difficult to obtain images along zones parallel with the cleavage plane.

We therefore also made specimens by ion beam thinning of polycrystalline specimens. Such specimens are extremely brittle. They were mainly used for diffraction studies but they were not thin enough for high-resolution work.

High-resolution images finally had to be obtained by patiently searching for suitably oriented cleavage fragments.

3. Structural Considerations

The structure of a typical representative of this series, corresponding to $n = 5$, is represented in Fig. 1 as projected along a $[11\bar{2}0]$ zone of the hexagonal unit cell (*2*). Along the c direction one layer of As_2Te_3 alternates with five layers of GeTe leading to a c parameter of

$$1 \times 1.011 \text{ nm} + 5 \times 0.349 \text{ nm} = 2.76 \text{ nm}.$$

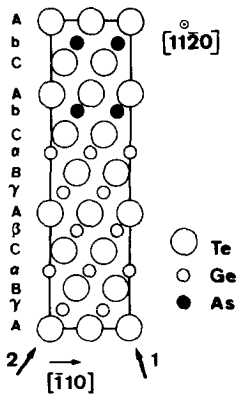

FIG. 1. Schematic representation of the structure of a typical representative of the series of homologous compounds. $As_2Te_3(GeTe)_n$ with $n = 5$ as projected along the $[11\bar{2}0]$ zone.

The same building principle applies to the other compounds; in all of them a single As_2Te_3 layer alternates with a slab of n GeTe layers. The resulting structures belong to the space group $P\bar{3}m1$ or $R\bar{3}m$. They can also be referred to a hexagonal cell with its basal plane parallel to the layer plane. The structure can to a good approximation be represented by the stacking of close-packed tellurium layers with the arsenic and the germanium atoms in octahedral interstices.

The stacking symbol for the compound $(As_2Te_3)(GeTe)_5$ would then be

$$\begin{matrix} A\gamma B\alpha C\beta A\gamma B\alpha & CbACb\ A\gamma B \\ 5\text{GeTe} & As_2Te_3. \end{matrix} \quad \ldots \quad (1)$$

The capital letters represent tellurium layers, the Greek letters germanium atoms, and the small Latin letters represent arsenic atoms.

The GeTe lamellae consist of Te layers stacked in the cubic fashion, the germanium atoms being located in the octahedral interstices. In the As_2Te_3 lamella the tellurium layers are stacked in the hexagonal fashion, the arsenic atoms being located again in the octahedral interstices within this lamella; the stacking of the tellurium atoms is thus cubic apart from two triplets in the hexagonal mode. Only two layers of interstices in the hexagonal triplets are filled; the central one is empty. The bonding is probably weakest at this level; it is to be expected that cleavage will preferentially take place along the plane separating the two tellurium layers.

The two types of lamellae occurring in this compound have structures closely related to the structures of the pure compounds GeTe and As_2Te_3.

Pure GeTe has a slightly deformed sodium chloride structure; it is rhombohedral

with its threefold axis perpendicular to the layer planes. The (111) planes of this structure are thus parallel with the (0001) plane of this family of mixed layer compounds.

The pure As_2Te_3 compound, which is stable at room temperature, has a complicated monoclinic structure, which has no simple relationship with the structure present in the As_2Te_3 lamellae. However, on moderately rapid cooling As_2Te_3 crystallizes in a structure which is metastable and which has a stacking based on a hexagonal stacking of the tellurium atoms with the arsenic atoms in octahedral interstices: *AcBAcBcABc* . . . This structure transforms on annealing into the stable monoclinic structure mentioned above.

It is obvious that in the mixed layer compounds one of the lamellae of this metastable structure is present in epitaxy on GeTe, the orientation relationship being

$$(111)_{GeTe} \equiv (0001)_{As_2Te_3}.$$

The presence of a layer of As_2Te_3 introduces a displacement between successive GeTe lamellae which is to a good approximation the same as that introduced by the presence of an intrinsic stacking fault in a cubic stacking of GeTe layers. This can be deduced immediately from the stacking symbols of (1)–(4).

4. Symmetry Considerations

The symmetry of the resulting stacking depends on the number n of GeTe layers within one repeat. Three different classes of structures have to be considered:

$n = 3p - 1; n = 3p; n = 3p + 1; p =$ integer.

We have represented a basic stacking sequence for each of these classes:

$n = 2$: *AγBα CbACb|Aγ* . . . hexagonal (2)

$n = 3$: *AγBαCβ AcBAc BαCβAγ BaCBa CβAγBα CbACb|Aγ* . . . (3)
↑ ↑ ↑ Rhombohedral I

$n = 4$: *AγBαCβAγ BaCBa CβAγBαCβ AcBAc BαCβAγBα CbACb|Aγ* . . . (4)
↑ ↑ ↑
Rhombohedral II

Adding three more GeTe layers to the GeTe lamellae does not change the type of layer on which the As_2Te_3 layer has to be fitted; as a result the symmetry of the arrangement remains the same. In the rhombohedral forms the stacking sequence only repeats after three lamellae.

We conclude that the compounds with $n = 3p - 1$ are hexagonal and contain n GeTe and one As_2Te_3 layers in the unit cell. The compounds with $n = 3p$ are rhombohedral and contain $3 \times (n\text{GeTe} + 1\ As_2Te_3)$ layers in the unit cell. The stacking of the first layers in three successive lamellae, as indicated by arrows in the sequence (3) is ABC.

The compounds with $n = 3p + 1$ are also rhombohedral and contain again $3 \times (n\text{GeTe} + 1\ As_2Te_3)$ layers in the unit cell. The stacking of the first layers of the successive lamellae is now *ACB* (4), i.e., the order is reversed as compared to the other rhombohedral stacking.

The rhombohedral I and rhombohedral II structures can in principle be distinguished from the geometry of the diffraction pattern. The reciprocal lattice formed by the basic spot positions is determined by the stacking sequence *ABC* . . . of the basic structure. Inverting this sequence, i.e., making it *ACB* . . . would lead to the twin pattern.

Within the same basic structure the re-

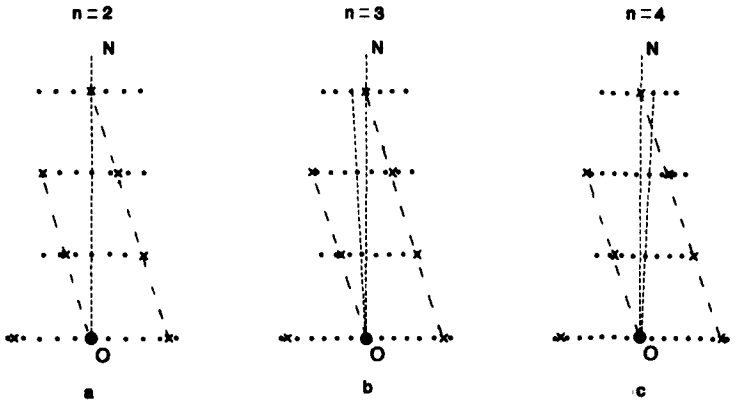

FIG. 2. Schematic representation of the diffraction patterns of the basic GeTe structure and of the mixed layer structures derived from this. (a) $n = 2$ (hexagonal); (b) $n = 3$ (rhombohedral I); (c) $n = 4$ (rhombohedral II).

ciprocal lattice of the long period rhombohedral structure is determined by the stacking sequence of the three blocks within the unit cell. This stacking is different for rhombohedral I and II as pointed out above and depends on n. The three possible cases are schematically represented in Fig. 2. Observed examples will be discussed below.

5. Diffraction Patterns

5.1. Geometrical Characteristics

The electron diffraction patterns of a representative member of this series along three important zones [0001], [11$\bar{2}$0], and [01$\bar{1}$0] of the same specimen are reproduced in Fig. 3. Figure 3a is a basal section; it is clearly compatible with the rhombohedral or hexagonal symmetry of these compounds.

The [01$\bar{1}$0] and [11$\bar{2}$0] zone patterns confirm the rhombohedral symmetry. When focussing attention on the positions of the most intense spots it becomes clear that these can be indexed on a rhombohedral lattice with $a = 0.401$ nm and $c = 0.349$ nm (in the hexagonal description). The most intense spots in successive dense rows of spots are shifted lengthwise over one-third (modulo 1) of the separation of the intense spots, which is consistent with a rhombohedral basic lattice. The exact distance between successive intense spots is somewhat ambiguous since sometimes two adjacent almost equally intense spots occur. However, in most cases it can clearly be divided in seven equal intervals. The long period corresponding with this satellite separation is $\approx$2.41 nm. This corresponds closely with 1.011 nm + 4 × 0.349 nm = 2.41 nm. Since the thickness of the As_2Te_3 lamella (1.011 nm) is roughly three times the thickness of a GeTe layer the superstructure unit cell has a "thickness" which is roughly seven times that of a GeTe layer. As a result if N is the number of satellite intervals in the distance between basic spots one has in the general case $n \approx N - 3$ (in this case $n = 4$). This approximation is better with the larger n values. The main maxima are all located at or close to positions which are compatible with the GeTe structure; this is due to the fact that the main constituent, especially for large n values, is GeTe.

The diffraction pattern exhibits all the characteristic features of mixed layer compounds consisting preponderantly of GeTe. The intensities of the first satellites decrease rapidly with their distance from the

basic GeTe positions, but nevertheless most other satellites remain visible.

The positions of the intense spots in the central row and in the third row of the [11$\bar{2}$0] zone diffraction patterns are not affected by the details of the stacking sequence; they can thus be used as reference positions which allow the determination of all the spot positions due to the rhombohedral basic structure.

We now focus attention on the superstructure spots (or satellites). It is evident from the scheme of Fig. 2 that the sequences of satellite spots have undergone a fractional shift of one-third (modulo 1) with respect to the basic spots.

By drawing a line ON perpendicular to the central row of satellites, one notes that three different patterns are present.

In one type of pattern the satellites in all rows are situated on this line; these compounds are hexagonal; an example is shown in Fig. 4a which corresponds with $N = 8$, i.e., $n = 5$.

Figure 4c shows a second case where now the satellite spots are shifted laterally over one-third of the intrasatellite spacing to the left looking away from the origin along the line ON for the first row, one-third to the right for the second row, and no shift for the third row. This is a clear indication that the superstructure also has rhombohedral symmetry. We find $N = 6$ and hence $n = 3$ (a threefold).

In Fig. 4b on the other hand the lateral shifts of superstructure spots with respect to the line ON are one-third to the right for the first row, one-third to the left for the

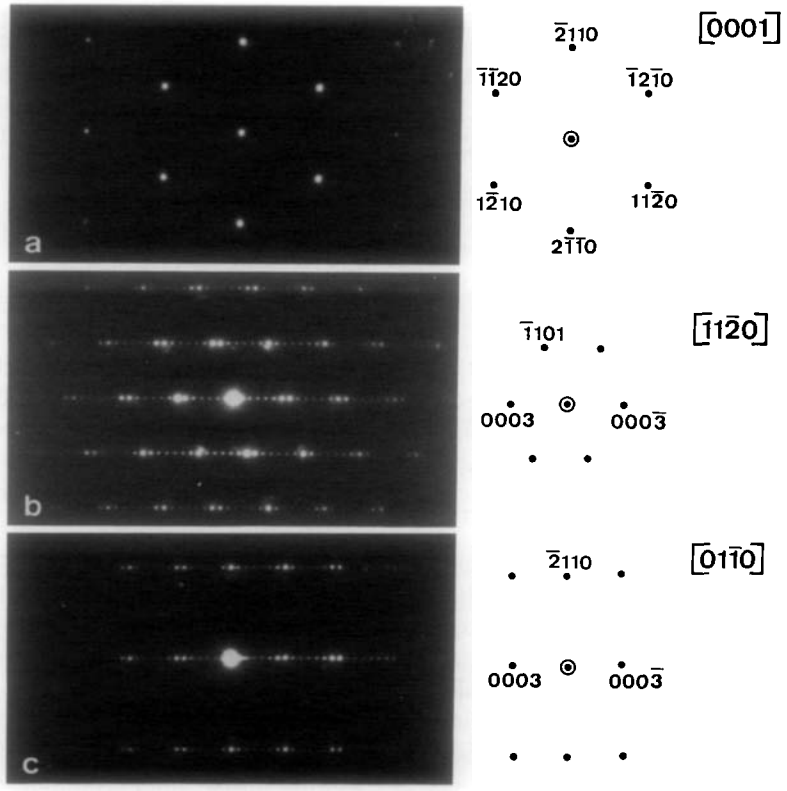

FIG. 3. Electron diffraction patterns along three representative zones of the compound with $n = 4$. (a) [0001] zone; (b) [11$\bar{2}$0] zone; (c) [01$\bar{1}$0] zone.

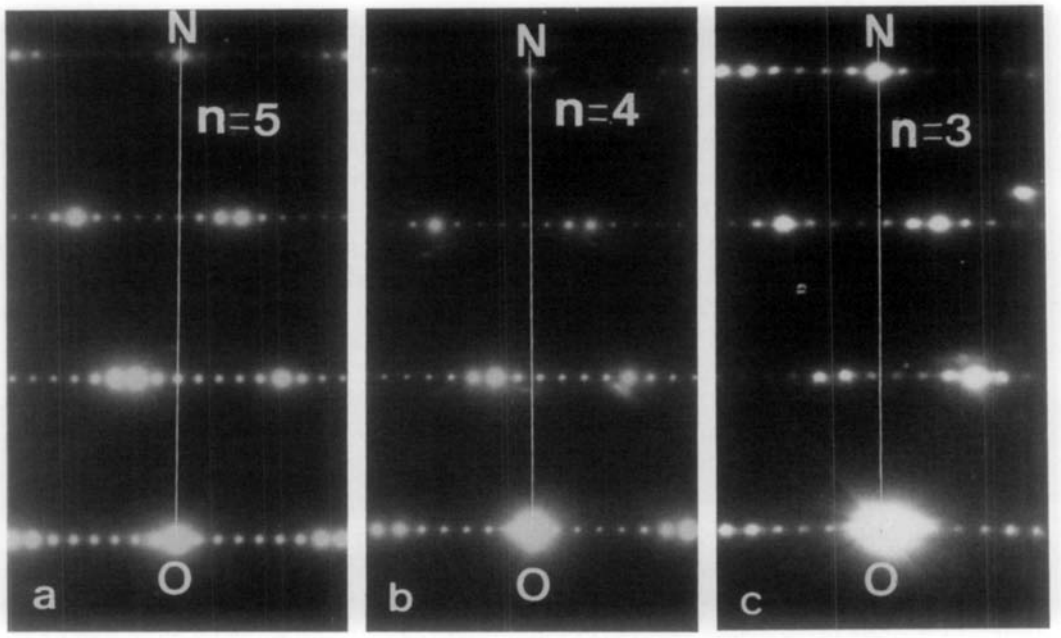

FIG. 4. Diffraction patterns of the hexagonal structure and of the rhombohedral I and rhombohedral II structures, based on the same basic GeTe structure. (a) Hexagonal ($n = 5$); (b) rhombohedral II ($n = 4$); (c) rhombohedral I ($n = 3$).

second row, and no shift for the third row, i.e., they are in the opposite sense as compared to the previous case. The superstructure has again rhombohedral symmetry. In this case $N = 7$ or $n = 4$ (i.e., $3p + 1$). The two rhombohedral diffraction patterns correspond with rhombohedral I and II structures, respectively.

The fractional shifts of the satellite sequences with respect to the basic spot positions are one-third (modulo 1) or zero in all cases. This is consistent with the fact that the net displacement caused by the presence of the As_2Te_3 layer in the GeTe cubic sequence is equivalent in all cases to that introduced by an intrinsic stacking fault.

5.2. Intensity Considerations

The rapid decrease of the first-order satellite intensity in the vicinity of the GeTe basic spots and the rather uniform low intensity of the remaining satellites is consistent with the structure, and in agreement with the predicted general features of diffraction patterns due to mixed layer compounds (*3*).

The rapid decrease of intensity and the larger intensity of the spots in the vicinity of the GeTe positions is due to the fact that GeTe is the main constituent and occurs as a "thick" lamella. On the other hand As_2Te_3 occurs as a thin lamella and thus the intensity of the spots in the vicinity of the As_2Te_3 positions is smaller and is spread out over several satellites (*3*). The As_2Te_3 spot positions divide two successive GeTe positions in three equal intervals. As a result the intermediate satellites are all of rather comparable intensity since they are all almost equally close to an As_2Te_3 position.

6. Stacking Variants

We have observed well-defined diffraction patterns corresponding with stacking

variants with $n = 3, 4, 5, 6, 7, 8, 9$ (see Figs. 4 and 5). All these variants follow the same building principle described above. Whereas the X-ray powder diffraction patterns suggested that variants with n up to 15 were formed (*1*) we found that for compositions corresponding with $n > 9$ the diffraction patterns of certain fragments exhibit stacking disorder, whereas most of the fragments in the $n = 18$ compound exhibit the pure GeTe diffraction patterns. We shall show that the structure is then better described as a GeTe matrix with one layer As_2Te_3 "precipitates" on the (111) planes.

7. *High-Resolution Images*

High-resolution images of the different members of the homologous series were produced along the [11$\bar{2}$0] zone including diffraction spots up to a spacing of 0.14 nm within the selection aperture. Along this zone one is viewing the structure along the close-packed rows of tellurium atoms. In Fig. 6a we have reproduced the image of a typical member ($n = 5$) of the series. The rhombohedral stacking in the thick GeTe lamella is clearly revealed by the configuration of bright dots. Also the thin As_2Te_3 lamellae are revealed as a local hexagonal stacking of bright dots. These conclusions are independent of the imaging code, which can only be deduced by computer simulations (see Section 8).

When viewing the images along direction 1 indicated in Fig. 6a the rows of bright dots are laterally shifted on crossing the As_2Te_3 lamellae due to the presence of the intrinsic faults, whereas they are only slightly perturbed along direction 2. This is consistent with the model of Fig. 1. The rows of tellurium atoms behave in the same way as the bright dots when viewing the model along directions 1 and 2. The inset of Fig. 6a, which is a model of the structure with $n = 5$

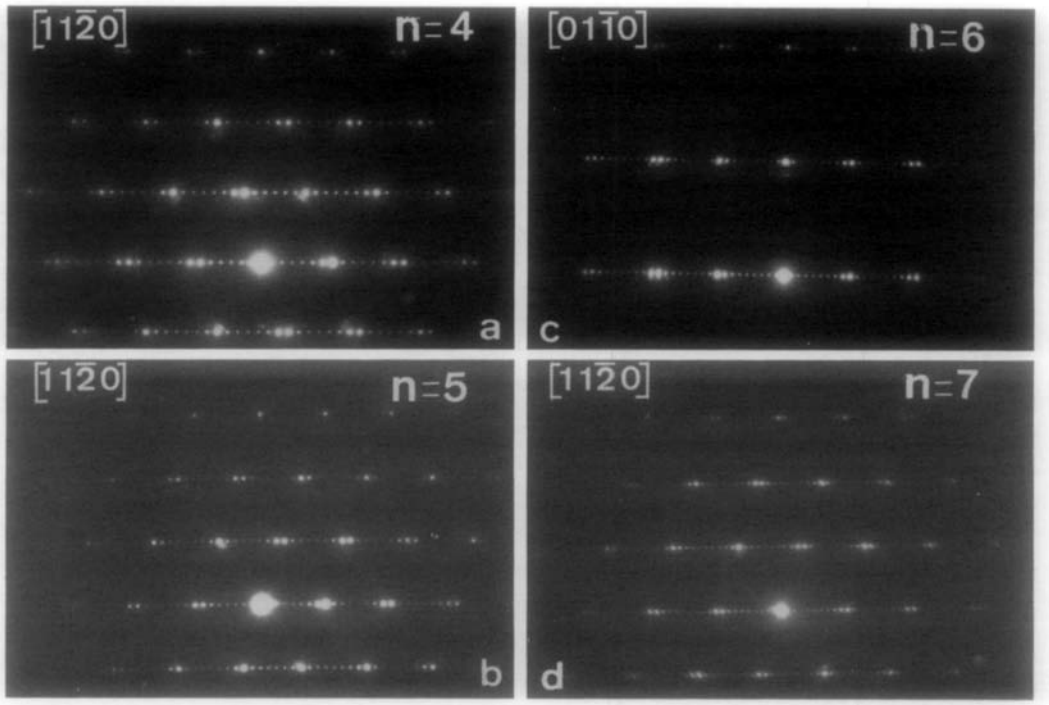

FIG. 5. Diffraction patterns of four different members of the homologous series $As_2Te_3(GeTe)_n$: (a) $n = 4$ [11$\bar{2}$0] zone; (b) $n = 5$ [11$\bar{2}$0] zone; (c) $n = 6$ [01$\bar{1}$0] zone; (d) $n = 7$ [11$\bar{2}$0] zone.

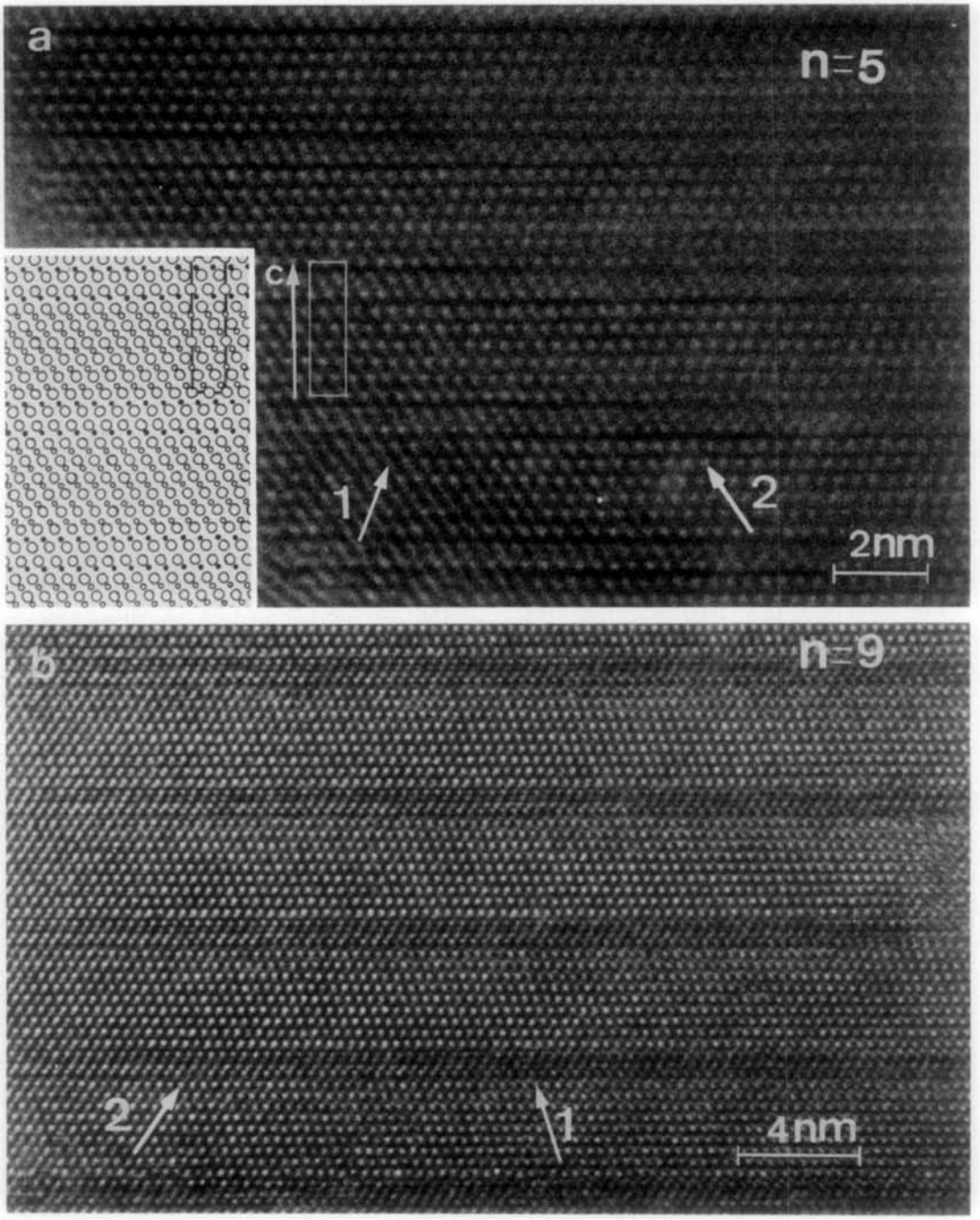

FIG. 6. High-resolution images viewed along a close-packed direction of the tellurium sublattice of the compounds with $n = 5$ (a) and $n = 9$ (b). Note the rhombohedral stacking of the tellurium atoms in the GeTe lamella and the hexagonal stacking in the As_2Te_3 layer. The inset is a structure model for $n = 5$ at the same scale. Along direction 1 the rows of bright dots suffer an offset along the As_2Te_3 lamella, but not along direction 2.

drawn at the same scale as the image illustrates this very clearly.

Other high-resolution images corresponding with $n = 9$ and a mixture of 8 and 9 are reproduced in Figs. 6b and 7, respectively.

Figure 8a shows a one-dimensional fringe pattern of a compound with $n = 18$. We have intentionally chosen to reduce the image detail by selecting only spots along a single row in order to be able to image a larger area and nevertheless obtain the required information. The corresponding diffraction pattern exhibits considerable streaking along the rows of superstructure spots (inset of Fig. 8a). The image shows extensive fringe patterns with a spacing corresponding with GeTe interrupted by singular often ending fringes with a somewhat larger spacing.

The singular fringes have a variable separation, the average being around 12 interfringe spacings. We believe that the singular fringes represent in fact single As_2Te_3 layers or precipitates which are irregularly spaced and which do not extend throughout the whole layer plane. A given layer of octahedral interstices may in certain regions be filled with arsenic and in other regions with germanium. The parts filled with arsenic would give rise locally to a somewhat wider fringe spacing. The diffraction pattern of such a specimen may still produce diffraction maxima corresponding with the average spacing of such one layer As_2Te_3 precipitates. This assumption may explain why X-ray powder diffraction patterns still reveal diffraction maxima which can be ascribed to compounds with $n > 9$, whereas we have not found well-defined single-crystal electron diffraction patterns of the members with $n > 9$.

Locally the separation of the layer planes as imaged by lattice fringes is somewhat larger as can be seen by viewing along the layer planes. The limits of the As_2Te_3 single layer platelets are partial dislocations of a peculiar type with a Burgers vector which

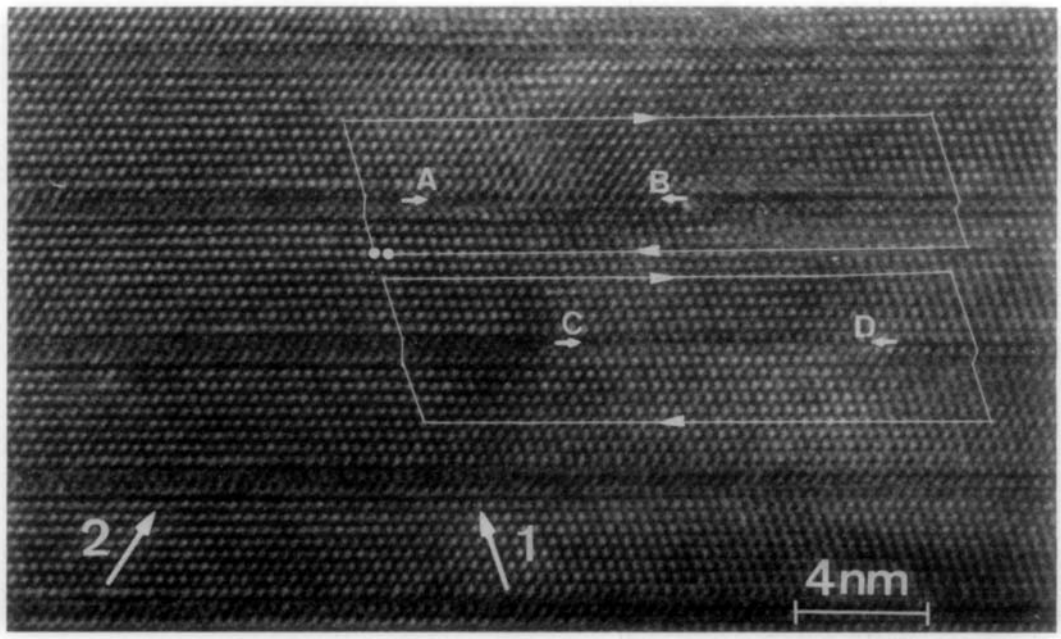

FIG. 7. High-resolution image along a close-packed direction of the tellurium sublattice corresponding with the compound $n = 9$. Note the presence of planar defects along *AB* and *CD*.

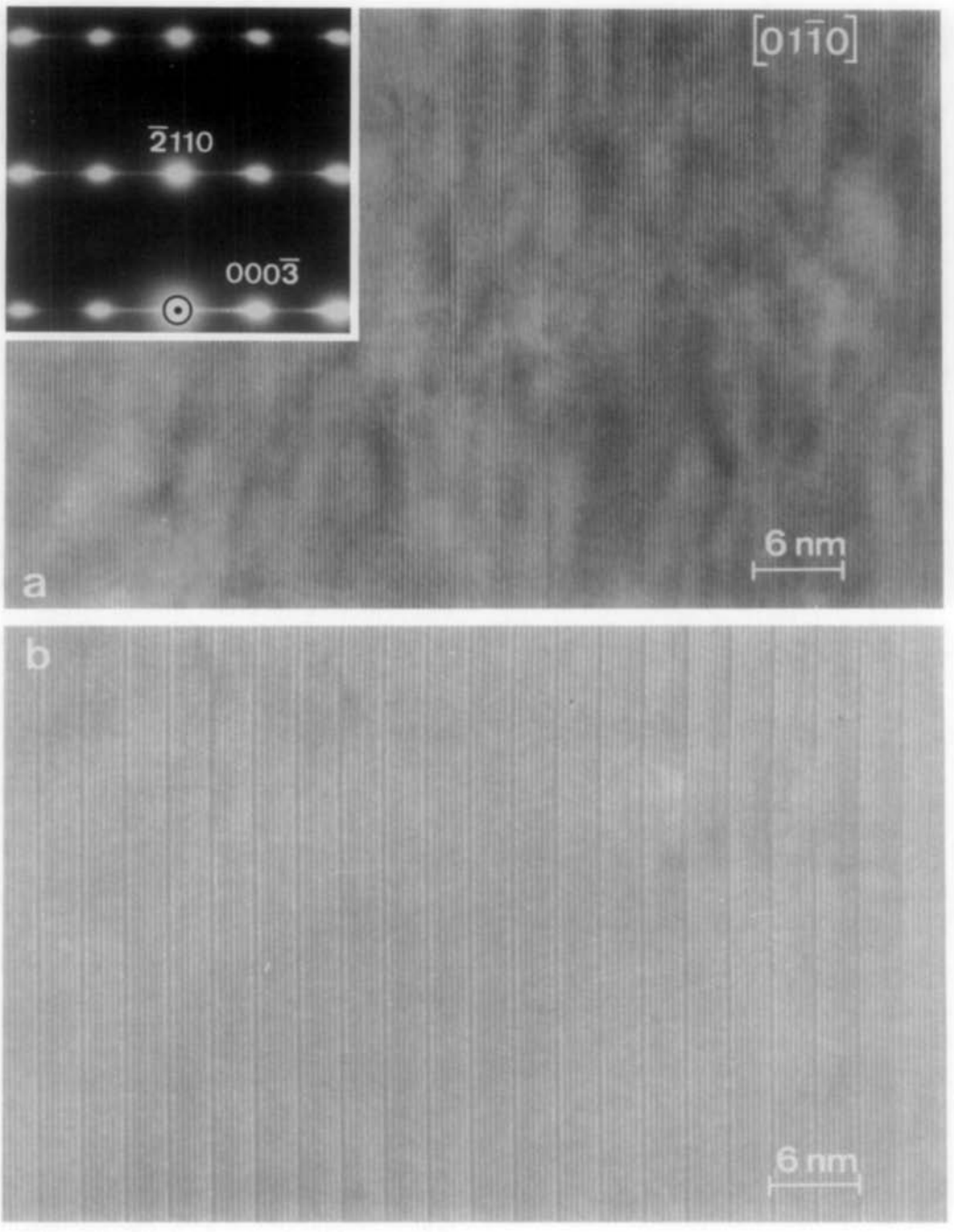

FIG. 8. One-dimensional lattice fringes. (a) Irregular fringes: observed along the $[01\bar{1}0]$ zone in the compound with $n = 18$. The inset shows the diffraction pattern of such a specimen. (b) Periodic fringes: observed along the $[01\bar{1}0]$ zone in the compound with $n = 5$.

is not related in a simple manner to the lattice of either GeTe or As_2Te_3.

A model for such a terminating lamella is represented in Fig. 12.

In Fig. 8b we have reproduced one-dimensional lattice fringes for a periodic compound with $n = 5$, taken along the $[01\bar{1}0]$ zone. It can be compared with the irregular fringe patterns discussed above; in particular it allows the identification of the broader fringes with thin As_2Te_3 lamellae.

8. Image Simulation

The images of a typical member of the series $n = 5$ were computer simulated using the direct space method developed by Coene and Van Dyck (*4*). The coordinates of the atoms were those determined by Han Wan Shu *et al.* (*1*). The spherical aberration constant was $C_s = 1.2$ mm, the beam divergence 8×10^{-4} rad, the focus spread 7 nm, and the accelerating voltage 200 kV.

Images were calculated along the $[11\bar{2}0]$ zone for different thicknesses t ranging from 4 to 20 nm and for defocusing values Δ ranging from -20 to -140 nm. Scherzer defocus is at about -66 nm. The matrix of images is reproduced in Fig. 9. The best fit with the observed images is obtained for a defocus of -20 nm and for a thickness of 8.2–20 nm. The origin in the left bottom corner was chosen in a tellurium position of the model of Fig. 1. Under these conditions the bright dots can thus be considered to be the images of tellurium columns.

Viewing the computed images along directions 1 and 2 we find the same features as those observed on the actual images by viewing along the directions numbered correspondingly in Fig. 6. We can conclude that the observed images confirm fully the structures determined by X-ray diffraction.

9. Dislocations

Diffraction contrast images show that the crystals deform by glide along the basal plane. Because the bonding is weakest between the two adjacent close-packed tellurium layers in the As_2Te_3 lamella, slip is expected to take place along the plane separating these two layers. The dislocations are invariably found to be coupled in wide ribbons (Fig. 10). The dislocations are thus clearly dissociated in Shockley partials, as one would expect for glide between close-packed layers. The stacking fault energy is small; for the width of the ribbons one finds $d = 27$ nm. From the geometry of the close-packed Te layers one can conclude that $b = 0.24$ nm and assuming a reasonable value for $\mu = 10^{-10}$ N/m^2 one finds $\gamma \sim 5\text{–}6 \times 10^{-3}$ J/m^2 which is rather small (*5*).

Some of the high-resolution images give direct evidence for the occurrence of stacking faults limited by partial dislocations within the As_2Te_3 lamella. When viewing Fig. 7 along direction 1 it is clear that the rows of bright dots undergo an offset along the As_2Te_3 lamella except in the parts between the two arrows where no offset is present. Assuming that a stacking fault of the type that would be produced in the wake of a Shockley partial is present along the As_2Te_3 lamella, the stacking would become as is represented in Fig. 11 and no offset of the tellurium rows would occur. It is therefore suggested that the absence of an offset is in fact due to the presence of a dislocation ribbon in the central plane of the As_2Te_3 lamella.

If we make a Burgers circuit around the segment *AB* along which there is no offset, we find that it is not closed, the closure failure being the distance between two bright dots. This closure failure is the projection along the close-packed rows of the Burgers vector of a perfect dislocation, which is consistent with the assumption that *AB* is the section of a ribbon.

There is one apparent difficulty, the distance between partials observed in Fig. 7 is much smaller than the distance deduced from the image of Fig. 10. However this is

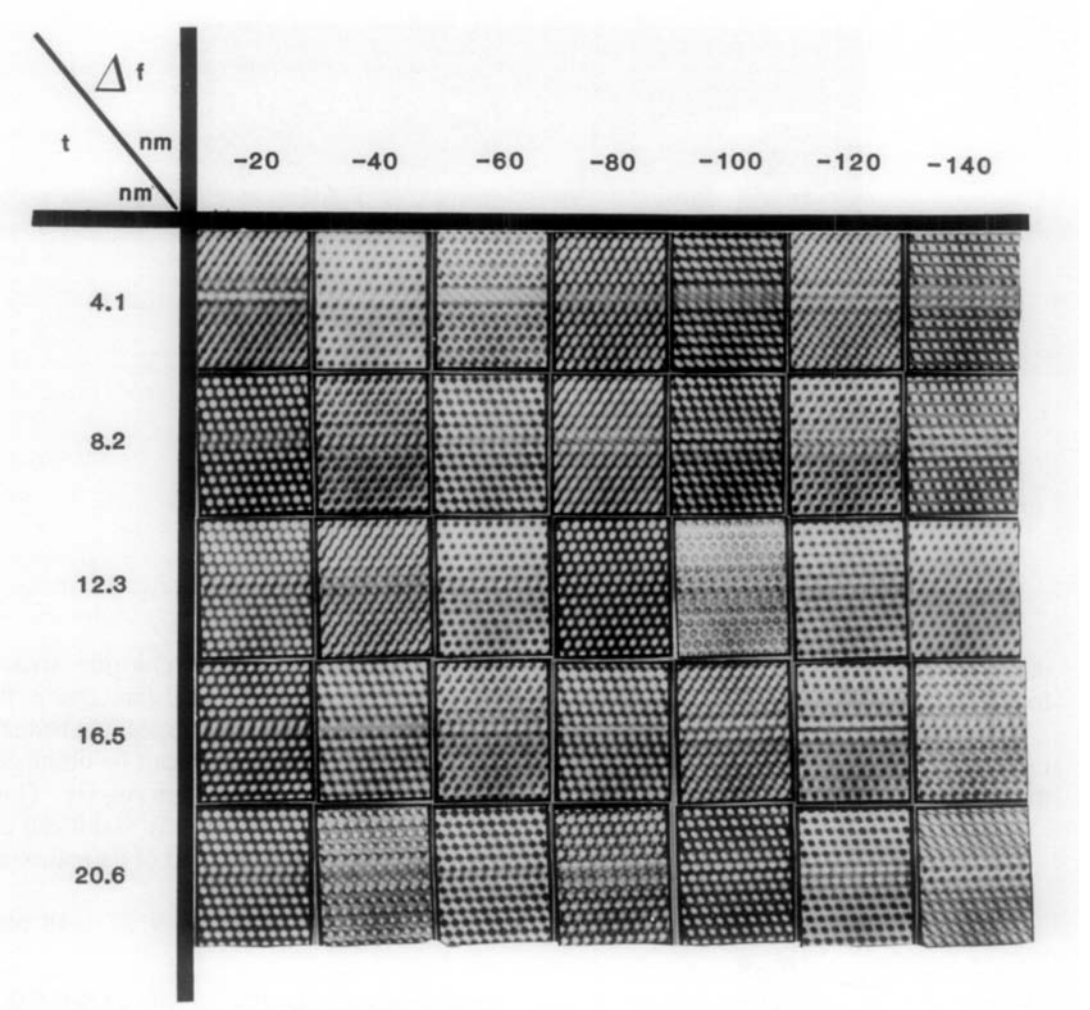

FIG. 9. Matrix of simulated images along the [11$\bar{2}$0] zone for different thicknesses (t) and defocus values (Δ) (C_s = 1.2 mm; beam divergence 8×10^{-4} rad; focus spread 7 nm; accelerating voltage 200 kV).

consistent with the fact that in the present case the crystal foil is extremely thin and much thinner than the foil that produced the image of Fig. 10. Thus the elastic interaction force, i.e., the repulsion between partial dislocations, is strongly reduced, whereas the attraction, due to the stacking fault, is not affected (*5*).

The Burgers circuit around *CD* on the other hand is closed; a possible model based on the presence of a "precipitate" of GeTe or a single layer of As is shown in Fig. 12 as well.

10. Discussion and Conclusions

The suggestion derived from X-ray diffraction experiments that the compounds As_2Te_3 $(GeTe)_n$ form a homologous series for n = 1 . . . 9 has been confirmed by electron diffraction and high-resolution

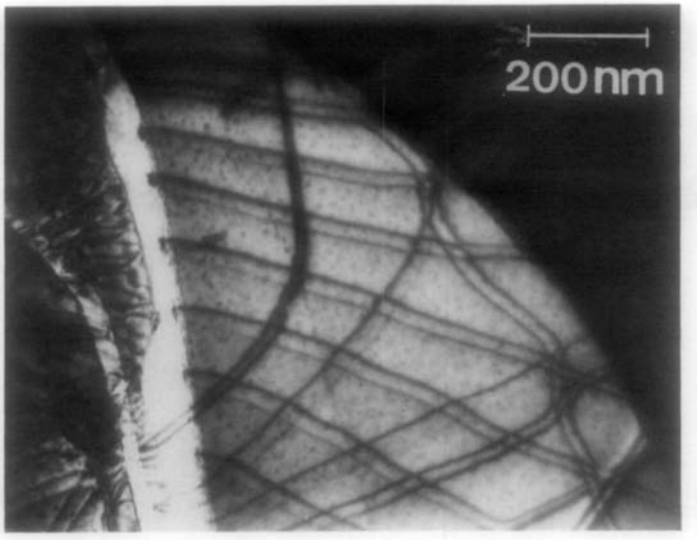

FIG. 10. Wide dislocation ribbons in the basal plane (0001).

imaging. The building principle is the same for all these compounds.

Regularly spaced As_2Te_3 lamellae containing two arsenic layers are inserted in the rhombohedral GeTe matrix which has a slightly deformed sodium chloride structure. The structure in these lamellae is in fact the same as that of a metastable hexagonal form of As_2Te_3 which can be obtained only on fast cooling of molten As_2Te_3. This crystal structure is apparently stabilized at room temperature as a result of its epitaxial relationship with GeTe.

The materials with $n > 9 \ldots 18$ are

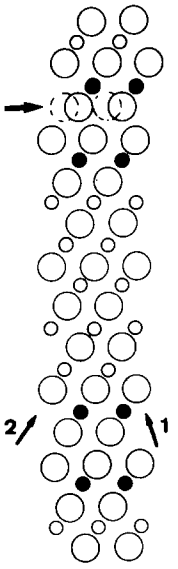

FIG. 11. Model for the stacking fault produced by the passage of a Shockley partial along the glide plane situated in the Van der Waals gap of the As_2Te_3 layer.

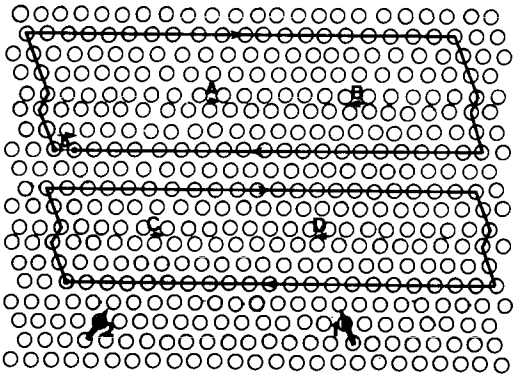

FIG. 12. Model for the local structure observed in Fig. 7. Along *AB* a stacking fault ribbon is present. This can be deduced from the closure failure of a Burgers circuit. Along *CD* the Burgers circuit is closed; *CD* is probably the trace of a one layer precipitate of arsenic.

found to be inhomogeneous. In most crystal fragments only the GeTe fringes can be detected, but in a fraction of them the GeTe fringes are quasiperiodically perturbed by somewhat wider fringes. It is suggested that they are due to the presence of As_2Te_3 lamellae which are somewhat irregularly spaced and possibly to monolayers of arsenic on the close-packed layers.

For arsenic concentrations corresponding with n values close to 9, the arsenic is regularly distributed in equally spaced bilayer lamellae. The fact that the arsenic layers become irregularly spaced and finally randomly spaced with decreasing arsenic concentration can be understood by assuming some repulsive interaction between such layers which decreases with increasing separation. At arsenic concentrations which exceed $n = 9$ the repulsion is apparently sufficient to keep the arsenic layers equally spaced but at still smaller concentrations corresponding to $n > 9$ the repulsion becomes too small and only an average separation which increases with decreasing arsenic concentrations is realized; furthermore the arsenic lamellae do not extend over the whole lattice plane and may become monolayers in certain parts.

Acknowledgments

This work was performed in the framework of the Institute for Materials Science (IMS) of the University of Antwerp and financially supported by IIKW.

References

1. HAN WAN SHU, S. JAULMES, A. MAZURIER, AND B. OLLITRAULT-FICHET, *C. R. Acad. Sci. Paris* **302,** 557 (1986).
2. S. JAULMES, HAN WAN SHU, AND A. MAZURIER, *Acta Crystallogr.*, in press.
3. G. VAN TENDELOO, D. VAN DYCK, S. KUYPERS, AND S. AMELINCKX, *Phys. Status Solidi A* **101,** 339 (1987).
4. W. COENE AND D. VAN DYCK, *Ultramicroscopy* **15,** 41 (1984).
5. S. AMELINCKX, *in* "Dislocations in Solids" (F. R. N. Nabarro, Ed.), Vol. 2, p. 67, North-Holland, Amsterdam (1979).